BIOCHEMISTRY
including biophysical chemistry & molecular biology

Article

pubs.acs.org/biochemistry

Identification of a Hydrophobic Cleft in the LytTR Domain of AgrA as a Locus for Small Molecule Interactions That Inhibit DNA Binding

Paul G. Leonard,[†] Ian F. Bezar,[†,§] David J. Sidote,[†] and Ann M. Stock*[,†,‡]

[†]Center for Advanced Biotechnology and Medicine, [‡]Department of Biochemistry and Molecular Biology, and [§]Graduate School of Biomedical Sciences, University of Medicine and Dentistry of New Jersey-Robert Wood Johnson Medical School, Piscataway, New Jersey 08854-5635, United States

ABSTRACT: The AgrA transcription factor regulates the quorum-sensing response in *Staphylococcus aureus*, controlling the production of hemolysins and other virulence factors. AgrA binds to DNA via its C-terminal LytTR domain, a domain not found in humans but common in many pathogenic bacteria, making it a potential target for antimicrobial development. We have determined the crystal structure of the apo AgrA LytTR domain and screened a library of 500 fragment compounds to find inhibitors of AgrA DNA binding activity. Using nuclear magnetic resonance, the binding site for five compounds has been mapped to a common locus at the C-terminal end of the LytTR domain, a site known to be important for DNA binding activity. Three of these compounds inhibit AgrA DNA binding. These results provide the first evidence that LytTR domains can be targeted by small organic compounds.

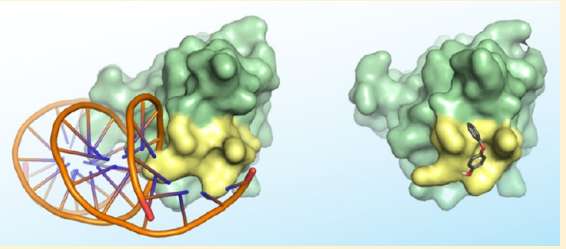

Staphylococcus aureus typically causes skin or soft tissue infections at a localized lesion.[1] Patients are at risk of more serious life-threatening diseases such as pneumonia, osteomyelitis, bacteremia, endocarditis, and toxic shock syndrome[2−5] if *S. aureus* is able to cross into the bloodstream. The treatment of *S. aureus* infections has become increasingly problematic because of the emergence of antibiotic resistant strains. Methicillin resistant *S. aureus* (MRSA) is now the most common antibiotic resistant pathogen identified in developed world hospitals[6] and poses a significant threat to human health.

The pathogenicity of *S. aureus* requires the coordinated expression of a large number of virulence factors. The *agr* quorum-sensing system, which allows the pathogen to sense both the density of the local *S. aureus* population and its degree of confinement, plays a central role in the regulation of the *S. aureus* virulon. Activation of the *agr* system represses the production of cell surface adhesins and promotes the secretion of extracellular toxins.

The *agr* operon consists of four genes, designated *agrBDCA*. The propeptide, AgrD, is processed and exported by AgrB. The secreted cyclic peptide is the autoinducing peptide (AIP) that functions as the quorum-sensing signal. When the extracellular AIP concentration is high, the histidine kinase, AgrC, is activated, resulting in an increased level of phosphorylation of the cytoplasmic response regulator protein, AgrA. Phosphorylated AgrA activates transcription of the *agrBDCA* operon, genes encoding phenol soluble modulins[7] and the effector RNA molecule, RNAIII.[8] In addition to its function as the mRNA for hemolysin *δ*,[9] RNAIII uses antisense RNA mechanisms to downregulate adhesins and activate the transcription of genes encoding hemolysins, Panton-Valentine leukocidin (PVL), and enterotoxins.[10−13]

Deletion of the *agr* operon attenuates the *S. aureus* infection in mouse and rabbit animal models of infection, demonstrating the importance of *agr* quorum sensing for pathogenesis.[14−19] Indeed, AIP analogues that inhibit the AgrC histidine kinase are effective in reducing the severity of *S. aureus* infection.[17,19] However, attempts to identify inhibitors of response regulator AgrA have not been reported, despite the attractiveness of AgrA as a target because of the absence of LytTR DNA-binding domain proteins in mammalian proteomes.[20]

We have determined the high-resolution crystal structure of the AgrA C-terminal LytTR domain ($AgrA_C$) and used a fragment screening approach to search for small molecule-binding sites on the DNA-binding surface of this domain. Fragment screening approaches have been widely used to efficiently screen a broad area of potential chemical space, using a relatively small library of compounds. Although the affinity of small fragment compounds for a target protein is expected to be relatively low, because of the low molecular weight of the compounds used (<300 g mol^{-1}), fragment screening can identify energetic focal points on a protein surface that can be targeted by small molecule compounds.[21]

EXPERIMENTAL PROCEDURES

Protein Expression and Purification. Unlabeled *S. aureus* $AgrA_C$ protein (AgrA residues Asp137−Ile238) samples were produced in *Escherichia coli* grown in terrific broth (TB) medium as previously described.[22] For NMR studies, isotopically ^{15}N-enriched and ^{15}N- and ^{13}C-enriched protein samples

Received: August 31, 2012
Revised: November 21, 2012
Published: November 26, 2012

of $AgrA_C$ were prepared by expressing the $AgrA_C$ protein in *E. coli* BL21(DE3) pLysS grown in M9 minimal medium at 18 °C using 2.5 g/L $(^{15}NH_4)_2SO_4$ and 2 g/L [^{13}C]glucose (Cambridge Isotope Laboratories) as appropriate. The M9 medium was supplemented with 50 μg/mL kanamycin, 50 μM $FeCl_2$, 2 μM $CuCl_2$, 2 μM Na_2MoO_4, 2 μM $NiCl_2$, 2 μM $CoCl_2$, 2 μM H_3BO_3, 10 μM $MnCl_2$, 10 μM $ZnSO_4$, 20 μM $CaCl_2$, and the following micronutrients (1 μM each): nicotininc acid, pyridoxine, thiamine, biotin, riboflavin, folic acid, D-pantothenic acid, and myoinositol. Recombinant protein expression was induced using 0.3 mM isopropyl β-D-thiogalactopyranoside.

All $AgrA_C$ protein samples were purified from *E. coli* lysates following the previously published procedure[22] using HiTrap SP HP cation exchange, HiLoad Phenyl Sepharose HP hydrophobic interaction, and HiLoad Superdex 75 gel filtration chromatography (GE Healthcare). Purified protein was transferred into appropriate buffers by dialysis.

Crystallization of $AgrA_C$. Initial $AgrA_C$ crystals were prepared at 4 °C by hanging drop vapor diffusion by mixing 1 μL of 1 mM $AgrA_C$ [dissolved in 20 mM Bis Tris, 100 mM NaCl, and 10 mM DTT (pH 6.0)] with 1 μL of reservoir solution [100 mM Tris, 150 mM $LiSO_4$, and 11% (w/v) PEG 4000 (pH 8.0)]. The hanging drop was suspended above a 1 mL reservoir. The crystals were improved by being streak seeded after incubation for 24 h under the same condition except the PEG 4000 concentration was lowered to 8% (w/v).

Data Collection and Structure Refinement. $AgrA_C$ crystals were soaked for 30 s in 50 mM Tris, 75 mM $LiSO_4$, 8% PEG 4000, and 20% glycerol (pH 8) before being flash-frozen in liquid nitrogen. A native data set was collected at 100 K using a Rigaku MicroMax-007 HF generator equipped with an RAXIS-IV^{++} detector. Data were processed and scaled with DENZO and SCALEPACK.[23] The structure of apo $AgrA_C$ was determined by molecular replacement using Phaser 2.0[24] with the DNA-bound state of $AgrA_C$ as the search model (Protein Data Bank entry 3BS1). The *R* factor after rigid body refinement of the best molecular replacement solution was 0.440. From the initial molecular replacement solution, the structure was rebuilt from scratch using RESOLVE[25] before iterative refinement using COOT 6.02[26] and Phenix.[27] The refined model contains two molecules of $AgrA_C$ within the asymmetric unit; chains A and B contain residues Glu141−Ile238 and Ser139−Ile238, respectively. The model was refined to 1.52 Å with *R* factor and R_{free} values of 0.180 and 0.209, respectively. All residues lie within the allowed regions of the Ramachandran plot and exhibit favorable bond angles and bond lengths. An overview of the data collection and refinement statistics is provided in Table 1.

NMR Spectroscopy. All NMR data were acquired on Varian INOVA 600 MHz or Varian 500 MHz spectrometers equipped with triple-resonance probes. The NMR spectra were referenced to an internal 4,4-dimethyl-4-silapentane-1-sulfonic acid (DSS) standard as described previously.[28] All spectra were processed using NMRpipe[29] and analyzed using CCPNMR analysis 2.1.[30]

For the backbone NMR assignments, ^{1}H−^{15}N HSQC,[31] HNCACB, HN(CO)CACB, HNCA, HN(CO)CA, and HNCO[32] spectra were recorded at 298 K from a sample containing 1 mM $AgrA_C$ in 20 mM sodium phosphate, 100 mM NaCl, and 5% D_2O (pH 5.8). The backbone resonance assignments for $AgrA_C$ were established for all residues between Asn138 and Ile238 except for Tyr229.

Table 1. X-ray Data Collection and Refinement Statistics (molecular replacement)

	$AgrA_C$[a]
Data Collection	
space group	$P2_12_12_1$
cell dimensions	
a, *b*, *c* (Å)	41.4, 45.9, 112.1
α, *β*, *γ* (deg)	90.0, 90.0, 90.0
resolution range (Å)	25.00−1.52 (1.55−1.52)[b]
R_{sym}[c]	0.045 (0.563)[b]
$I/\sigma(I)$	32.9 (2.0)[b]
completeness (%)	97.2 (89.8)[b]
redundancy	3.3 (2.7)[b]
Refinement	
resolution (Å)	20.72−1.52
no. of reflections	31964
data cutoff	$\sigma(F) > 0$
R_{work}[d]/R_{free}[e]	0.180/0.209
no. of atoms per asymmetric unit	
protein	1702
glycerol	18
water	254
average *B* factor (Å^2)	
protein	20.5
glycerol	32.3
water	32.6
rmsd from ideality	
bond lengths (Å)	0.006
bond angles (deg)	1.048

[a]A single crystal was used for the data collection. [b]Values in parentheses are for the highest-resolution shell. [c]$R_{sym} = \sum_h|I_h - \langle I\rangle|/\sum_h I_h$, where I_h and $\langle I\rangle$ represent the diffraction intensity values of individual measurements and the corresponding mean values, respectively. [d]$R_{work} = (\sum_h||F_o| - |F_c||)/\sum_h|F_o|$, where F_o and F_c are observed and calculated structure factor amplitudes, respectively. [e]R_{free} was calculated for 5% of the randomly selected reflections of the data set that were not used in the refinement.

^{15}N heteronuclear NOE[33] spectra were recorded with a 3.0 s ^{1}H saturation in the latter part of a 3.5 s preparation period delay, which was also used without radiofrequency pulses for the reference two-dimensional (2D) spectrum without NOEs.

A library of 500 fragment compounds (Maybridge Ro3 500 fragment library) was screened for binding to $AgrA_C$ using a WATERGATE W5 LOGSY NMR experiment.[34] Each sample contained a mixture of 10 compounds (400 μM each) and 15 μM $AgrA_C$, dissolved in 20 mM sodium phosphate, 100 mM NaCl, 10 mM DTT, and 5% D_2O (pH 7.0). As a negative control, spectra were acquired for a second sample without $AgrA_C$. Hit compounds were identified by the inversion of the compound spectra when $AgrA_C$ was present and validated using single-compound repeats of the WATERGATE W5 LOGSY experiment. The WATERGATE W5 LOGSY spectra were acquired at 20 °C using a mixing time of 1.2 s, 8192 complex data points, and a spectral width of 10000 Hz, with the number of scans set to 128. The acquisition time was 0.819 s with a relaxation delay of 3.0 s. The total experiment time was 11 min.

To identify the compound-binding sites, ^{1}H−^{15}N HSQC spectra were acquired for samples containing 300 μM $AgrA_C$ dissolved in 20 mM sodium phosphate, 100 mM NaCl, 10 mM DTT, and 5% D_2O (pH 5.8) after each addition of compound to the protein sample. Stock solutions (200 mM) of each compound, dissolved in DMSO-d_6, were used for the titrations.

dx.doi.org/10.1021/bi3011785 | *Biochemistry* 2012, 51, 10035−10043

A control experiment in which 3% DMSO-d_6 was added to the $AgrA_C$ NMR sample in the absence of compound was used to establish which chemical shift perturbations were compound-dependent.

The combined chemical shift was calculated for each amide resonance after the addition of compound, using the established method,[35] and mapped onto the apo $AgrA_C$ crystal structure using Pymol version 1.2r2. For each compound, the spectra obtained with the highest concentration of compound tested in the NMR titrations were used to determine the combined chemical shift perturbation.

Compound Docking. In silico docking of the compounds binding to $AgrA_C$ was performed using Autodock Vina.[36]

Inhibition Assays. The activities of five compounds as inhibitors of $AgrA_C$ DNA binding were tested using an electrophoretic mobility shift assay performed in the presence of increasing amounts of each compound (from 0 to 5 mM) to test whether the presence of compound inhibits the DNA binding activity of $AgrA_C$. A 19 bp DNA duplex was prepared by annealing 5′-ATTTAACAGTTAAGTATTT-3′ with its complementary oligonucleotide in 21 mM sodium phosphate, 105 mM NaCl, and 10.5 mM DTT (pH 5.8) and purified by size exclusion chromatography using a Superdex 75 HR column. Solutions were prepared containing 2 μM DNA duplex, 20 μM $AgrA_C$, and various compound concentrations in 20 mM sodium phosphate, 100 mM NaCl, 10 mM DTT, and 2.5% DMSO-d_6 (pH 5.8). After incubation at room temperature for 30 min, 12% (w/v) Ficoll 400 was added to each sample to give a final concentration of 2% (w/v) before the samples were run on an 8% acrylamide/bisacrylamide, 40 mM Tris-HCl, 20 mM acetic acid, 1 mM EDTA (pH 8.0) (TAE) gel at 70 V and 4 °C. The gels were stained in TAE supplemented with 0.1 mg/mL ethidium bromide for 10 min prior to being destained in TAE for 10 min. DNA was visualized with UV light, and images were captured using a CCD camera imager (Alpha Innotech).

RESULTS

Backbone Resonance Assignments of $AgrA_C$. Backbone resonance assignments were determined for $AgrA_C$ using a ^{15}N- and ^{13}C-labeled sample of the AgrA LytTR domain (Asp137−Ile238). The protein sample gave excellent-quality NMR spectra with well-dispersed chemical shifts (Figure 1), allowing for assignment of the backbone resonances. Assignments could be made for all of the residues between Asn138 and Ile238 except for Tyr229, whose resonances could not be confidently assigned, probably because of overlapping cross-peaks with another amide cross-peak. The unusual downfield shift of the Ser202 backbone amide proton resonance is caused by the hydrogen bonding of this proton with the imidazole ring of His200, as observed in the crystal structure of $AgrA_C$. A similar downfield shift has been described for the hydrogen bonding of the Arg7 backbone amide to the His106 side chain in *Bacillus subtilis* chorismate mutase.[37]

$AgrA_C$ in the Absence of DNA. The structure of $AgrA_C$ bound to its target DNA duplex has been reported previously,[22] but any structural changes that occur within this domain upon DNA binding were unknown. To establish if there are structural differences between the apo and DNA-bound states of $AgrA_C$, both NMR and X-ray crystallographic analyses were used to investigate the structure of the $AgrA_C$ protein in the absence of DNA.

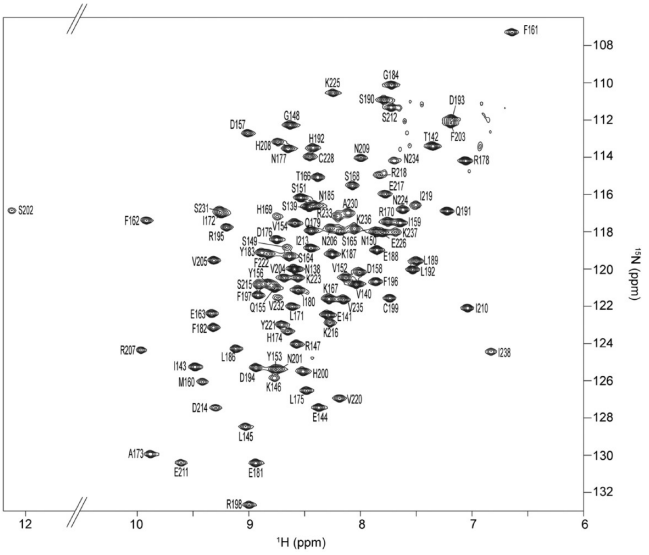

Figure 1. 2D $^{1}H-^{15}N$ HSQC spectrum of $AgrA_C$. Residue specific cross-peak assignments for the backbone amides are indicated.

$AgrA_C$ was crystallized in its apo state, forming $P2_12_12_1$ space group crystals that diffracted to 1.5 Å resolution. The structure of apo $AgrA_C$ was determined by molecular replacement. To remove model bias from the molecular replacement solution, the $AgrA_C$ protein was rebuilt from scratch using RESOLVE and then iteratively refined. The final structure contains two molecules of $AgrA_C$ in the asymmetric unit of the crystals (chain A contains Glu141−Ile238, and chain B contains Ser139−Ile238).

For both $AgrA_C$ protomers, the N-terminal residues are not observed in the electron density map, suggesting that this region is disordered, consistent with the negative $\{^{1}H\}-^{15}N$ heteronuclear NOE values observed for these amino acids (Figure 2A) under solution conditions. The apo $AgrA_C$ protein adopts a $\beta-\beta-\beta$ sandwich fold as observed previously for the DNA-bound state. The fold is stabilized by a set of conserved salt bridges: Glu141−Arg195, Asp157−His208, Asp193−Arg195, Asp157−Arg195, and His174−Glu226. The domain is very stable with heteronuclear NOE values for the backbone amide bond vectors between 0.7 and 1.0 for the majority of the protein. However, the $\beta1-\beta2$ loop, the $\beta3-\beta4$ loop, and the C-terminus have $^{1}H-^{15}N$ heteronuclear NOE values between 0.6 and 0.7, suggesting greater conformational flexibility for these regions than for the rest of the LytTR domain (Figure 2A). In addition, alternate rotamer conformations are observed in the electron density map for several amino acid side chains within the $AgrA_C$ crystal structure (Ser164, Ser215, and Glu217 from protomer chain A and Ile143, Ser149, and Asp176 from chain B), indicative of localized conformational flexibility within the domain. When the two protomer chains in the $AgrA_C$ crystal are superposed, the only differences in the protein backbone are observed for the N- and C-termini as well as the $\beta1-\beta2$, and $\beta3-\beta4$ loops, in excellent agreement with the heteronuclear NOE data. The rmsd for the two protomer chains in the apo $AgrA_C$ crystal is 0.19 Å for all backbone atoms, but a much greater difference is seen when the DNA-bound state is compared with apo $AgrA_C$ protein chain A or B (rmsd of 0.41 or 0.46, respectively), suggesting that a conformational change takes place upon DNA binding.

dx.doi.org/10.1021/bi3011785 | *Biochemistry* 2012, 51, 10035−10043

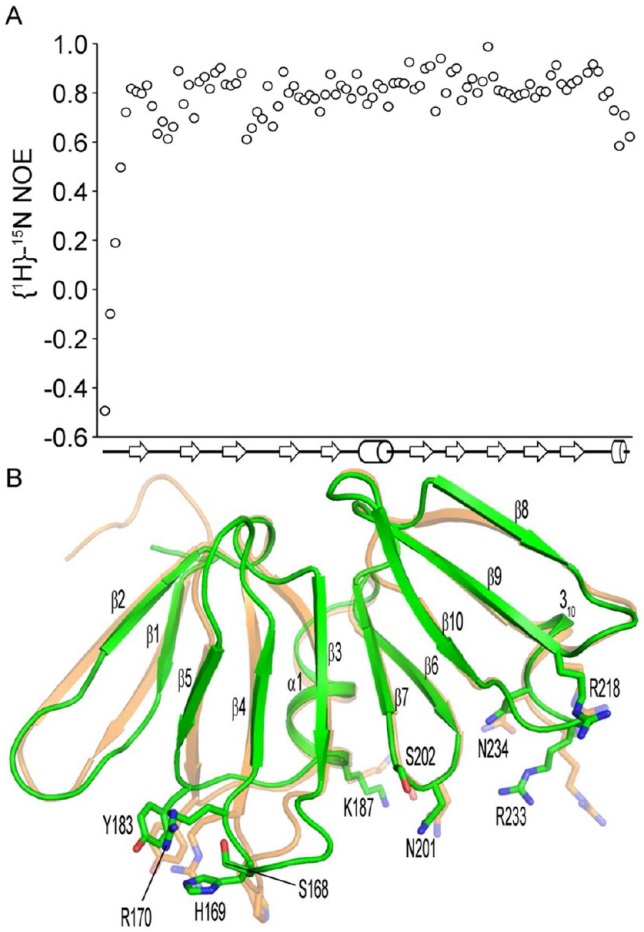

Figure 2. Conformational differences between apo and DNA-bound $AgrA_C$. (A) Steady-state heteronuclear $\{^1H\}-^{15}N$ NOE values for each residue of $AgrA_C$ plotted vs the secondary structure topology of the protein. β strands and α helices are depicted as arrows and cylinders, respectively. (B) Superposition of the apo $AgrA_C$ crystal structure (green) with $AgrA_C$ in its DNA-bound state (orange).[22] The side chains of amino acid residues within the DNA-binding surface that adopt different conformations between the apo and DNA-bound states are shown as sticks.

When the apo and DNA-bound structures of $AgrA_C$ are compared, changes in the conformation of the DNA-binding surface are observed for residues that are known to interact with the DNA backbone (Ser168, Arg170, Tyr183, Lys187, Ser202, Arg218, and Asn234) as well as three residues that make direct, base specific contacts (His169, Asn201, and Arg233)[22] (Figure 2B). The largest change between the DNA-bound and apo states of the $AgrA_C$ protein is observed for the $\beta3-\beta4$ loop (Ser165–Arg170). There are no crystal contacts for this region for the chain B protomer in the apo protein structure, so crystal lattice packing does not explain the different configuration of the $\beta3-\beta4$ loop relative to that in the DNA-bound state of $AgrA_C$. The conformational differences between the apo and DNA-bound structures suggest that DNA binding traps the protein into a conformation that represents only one conformation from the population of states adopted by the apo $AgrA_C$ protein. The conformational freedom of the DNA-binding surface would allow some flexibility for binding of AgrA to its DNA target sequences, albeit with an entropic penalty for binding.

Fragment Screening for Ligands of $AgrA_C$. LytTR domains are considered attractive drug targets for the development of new antibiotics because these domains are not present in humans and are often found to activate virulence pathways in bacterial pathogens.[20] NMR fragment screening methods were chosen because they allow the entire molecular surface of the target protein to be probed by a fragment compound library, in contrast to X-ray diffraction screening where some surfaces are occluded by lattice contacts. Fragment screening by NMR has proven to be a powerful tool for identifying regions of a protein that can be targeted by low complexity, small molecule ligands (fragment compounds), which subsequently can be used as starting points for drug development.[38,39] A library of 500 compounds was screened for binding to $AgrA_C$ using a WATERGATE W5 LOGSY NMR experiment. Five compounds, 4-phenoxyphenol, 9*H*-xanthene-9-carboxylic acid, 2-(4-methylphenyl)-1,3-thiazole-4-carboxylic acid, [5-(2-thienyl)-3-isoxazolyl]methanol, and 4-hydroxy-2,6-dimethylbenzonitrile, were identified as binding to $AgrA_C$ as indicated by inversion of the compound spectrum when $AgrA_C$ was present in the solution.

Mapping the Compound-Binding Site. Having identified five compounds that interacted with $AgrA_C$ in the initial screen, we titrated increasing amounts of each compound into a ^{15}N-labeled sample of $AgrA_C$ and monitored chemical shift perturbations in the $^{15}N-^1H$ HSQC spectrum of the protein (Figure 3). Addition of each of the five compounds resulted in the perturbation of the same chemical shifts corresponding to the backbone amides for residues Ser231, Val232, Arg233, Asn234, Lys236, Lys237, and Ile238, at the C-terminal end of the protein (Figure 4). A control experiment confirmed that the chemical shift perturbations were dependent on the presence of the compounds and not caused by the addition of DMSO-d_6 to the NMR sample (Figure 4F). Mapping the chemical shift perturbations onto the surface of $AgrA_C$ revealed a surface corresponding to a shallow groove formed by the $\beta10-\alpha2$ loop and helix $\alpha2$. Interestingly, the $\beta10-\alpha2$ loop is known to be important for binding of DNA by AgrA,[22] so ligands that occlude this site would be expected to reduce the DNA binding activity of AgrA.

Compound Binding Predictions. In silico docking was used to predict the binding mode of the compounds using AutoDock Vina.[36] The search box was restricted to the region at the C-terminal end of $AgrA_C$, identified by NMR as the binding site for the compounds (Figure 5). All five compounds docked into a shallow groove located between Val232 and Lys236. 4-Phenoxyphenol is predicted to form hydrogen bond interactions with Lys236 and the backbone carbonyl of Arg233 and bends around Val232 to make tight van der Waals interactions with this amino acid side chain. 9*H*-Xanthene-9-carboxylic acid binds with the planar xanthene ring structure between Val232 and Lys236. The predicted interaction is further stabilized by a salt bridge between the carboxylic acid group of the compound and the side chain amine of Lys236. 2-(4-Methylphenyl)-1,3-thiazole-4-carboxylic acid binding is predicted to be stabilized by a hydrogen bond between the thiazole nitrogen and the carbonyl group of Val232 and a salt bridge between Lys237 and the carboxylic acid group in the compound. [5-(2-Thienyl)-3-isoxazolyl]methanol is predicted to bind with the isoxazolyl ring oxygen forming a hydrogen bond with the Lys236 amine. The putative compound binding mode is further stabilized by a hydrogen bond between the Val232 backbone carbonyl group and the hydroxyl group of the

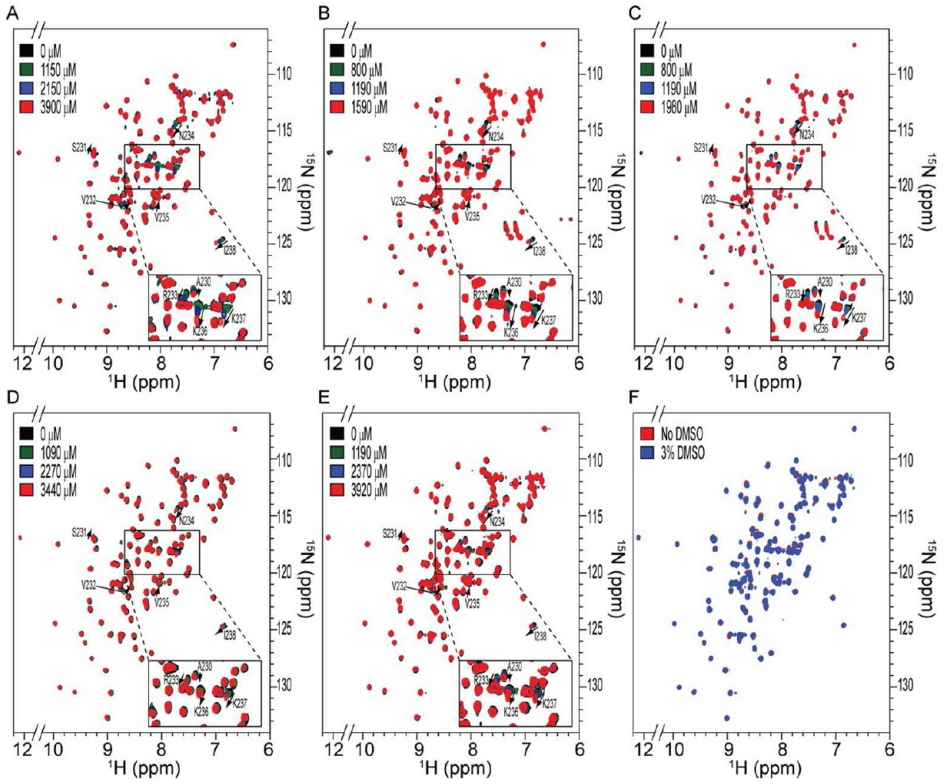

Figure 3. Chemical shift perturbations observed upon binding of fragment compounds to $AgrA_C$. $^{1}H-^{15}N$ HSQC spectra of $AgrA_C$ recorded in the presence of the indicated concentrations of (A) 4-phenoxyphenol, (B) 9*H*-xanthene-9-carboxylic acid, (C) 2-(4-methylphenyl)-1,3-thiazole-4-carboxylic acid, (D) [5-(2-thienyl)-3-isoxazolyl]methanol, and (E) 4-hydroxy-2,6-dimethylbenzonitrile. The residue specific assignments for backbone amide cross-peaks that shift in a compound concentration-dependent manner are highlighted. (F) $^{1}H-^{15}N$ HSQC spectra of ^{15}N-labeled $AgrA_C$ before and after the addition of 3% DMSO-d_6.

compound. The 4-hydroxy-2,6-dimethylbenzonitrile compound is predicted to bind in the shallow groove formed among Val232, Arg233, Lys236, and Lys237, with the hydroxyl group of the compound making hydrogen bond interactions with the backbone of Val232 and Lys236. The calculated binding energies for the best docking poses for 4-phenoxyphenol, 9*H*-xanthene-9-carboxylic acid, 2-(4-methylphenyl)-1,3-thiazole-4-carboxylic acid, [5-(2-thienyl)-3-isoxazolyl]methanol, and 4-hydroxy-2,6-dimethylbenzonitrile were −4.1, −4.1, −4.0, −3.5, and −3.6 kcal/mol, respectively, in agreement with the millimolar affinity observed by NMR.

Three Fragment Compounds Inhibit the DNA Binding Activity of $AgrA_C$. The five compounds identified by fragment screening all target the C-terminal end of $AgrA_C$, a region known to be involved in DNA binding.[22] It was therefore important to establish whether the compounds alter the DNA binding activity of AgrA. The DNA binding activity of $AgrA_C$ was tested using electrophoretic mobility shift assays in the presence of various compound concentrations from 75 to 5000 μM (Figure 6). For three compounds [4-phenoxyphenol, 9*H*-xanthene-9-carboxylic acid, and 2-(4-methylphenyl)-1,3-thiazole-4-carboxylic acid], the intensity of the band corresponding to the $AgrA_C$·DNA complex decreases as the compound concentration is increased; no $AgrA_C$·DNA complex is observed when 5 mM compound is present. Two other compounds {[5-(2-thienyl)-3-isoxazolyl]methanol and 4-hydroxy-2,6-dimethylbenzonitrile} had no apparent effect on the DNA binding activity of $AgrA_C$ at concentrations up to 5 mM. The DMSO concentration in all binding reaction mixtures was constant, so the disruption to the DNA binding activity of $AgrA_C$ is dependent only on the presence of the compound. In the control experiments without $AgrA_C$, there is no effect of the compounds on the migration of DNA through the gel. Some of the compounds that were identified to bind at the C-terminus of $AgrA_C$ can disrupt AgrA DNA binding activity.

DISCUSSION

The *agr* quorum-sensing system has been suggested as a possible drug target because deletion of the *agr* system attenuates *S. aureus* virulence in animal models of infection.[14−16,18] Furthermore, a functional *agr* system has been found to be important for bacterial survival in the early stages of abscess formation in animal models.[19] On the other hand, isolation of *agr*-deficient mutants from patients with chronic *S. aureus* infections[40] suggests that *agr* is not important for maintaining the infection once it has been established. Thus, substantial controversy surrounds the validity of the *agr* system as a target for antimicrobial drug development. *agr* inhibitors would be especially useful tools in addressing the role of the *agr* system during the course of infection in animal models of infection. Furthermore, *agr* inhibitors might be effective for prophylactic treatment. Indeed, co-inoculation of *S. aureus* with an *agr* inhibitor was sufficient to reduce virulence in a mouse skin infection model.[19]

To date, research on inhibitors of *S. aureus agr* quorum sensing has focused on analogues of the autoinducing peptide as inhibitors of AgrC activation.[17,19,41−43] Targeting *agr* quorum sensing using AIP analogues is complicated by the existence of several staphylococcal AgrC types that are inhibited or activated by different AIP molecules.[17,44,45]

dx.doi.org/10.1021/bi3011785 | *Biochemistry* 2012, 51, 10035−10043

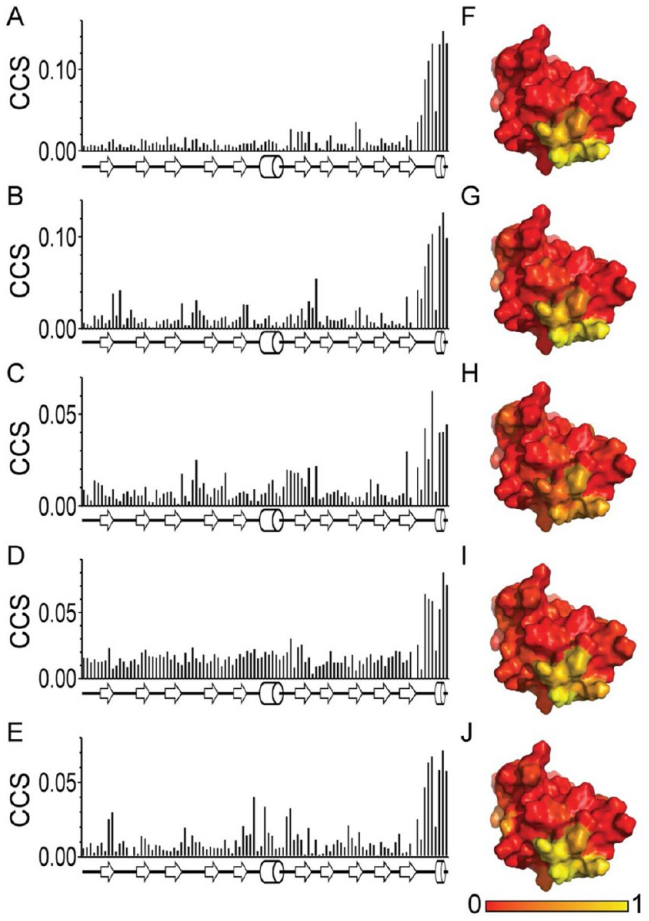

Figure 4. Mapping the compound-dependent chemical shift perturbations. Combined chemical shift perturbations of backbone amide resonances plotted vs the amino acid residue number for the addition of (A) 4-phenoxyphenol, (B) 9*H*-xanthene-9-carboxylic acid, (C) 2-(4-methylphenyl)-1,3-thiazole-4-carboxylic acid, (D) [5-(2-thienyl)-3-isoxazolyl]methanol, and (E) 4-hydroxy-2,6-dimethylbenzonitrile. The normalized combined chemical shift perturbations for (F) 4-phenoxyphenol, (G) 9*H*-xanthene-9-carboxylic acid, (H) 2-(4-methylphenyl)-1,3-thiazole-4-carboxylic acid, (I) [5-(2-thienyl)-3-isoxazolyl]methanol, and (J) 4-hydroxy-2,6-dimethylbenzonitrile are mapped onto the surface of the crystal structure of apo $AgrA_C$ with the region showing the greatest combined chemical shift perturbation colored yellow.

The results presented here represent the first attempt to inhibit the *agr* quorum sensing pathway by targeting the DNA-binding surface of the AgrA LytTR domain. Fragment screening can be used to identify an energetic focal point on the surface of a protein that is favorable to compound binding.[21] While small fragments are efficient in covering large areas of chemical space and have advantages as starting points for drug development, their binding affinities are typically very low. Indeed, only three of the five compounds that were identified as binding to $AgrA_C$ by NMR analyses disrupted DNA binding in electrophoretic mobility shift assays. For these compounds, inhibition was detected only at millimolar concentrations. The low affinity of ligand binding provides a likely explanation for the lack of inhibition observed with the other two compounds.

The five compounds identified by fragment screening as $AgrA_C$ inhibitors all bind to a highly conserved region that forms a short helix at the C-terminus of the AgrA protein. There are 211 AgrA protein sequences spread across all staphylococcal strains in the Uniprot knowledgebase database. Conservation of 100% sequence identity is observed for Ser231, Val232, Arg233, Asn234, Lys236, and Lys237 that are identified as residues in the compound-binding site. Val235 is conserved in 97% of all staphylococcal sequences, although isoleucine or leucine amino acids are observed at this position in *Staphylococcus siminae*, *Staphylococcus pseudintermedius*, *Staphylococcus intermedius*, and *Staphylococcus carnosus* strains. The C-terminal isoleucine residue (Ile238) is conserved in 94% of the AgrA protein sequences but is replaced with a lysine in *S. aureus* Mu3 and Mu50 strains or valine in *Staphylococcus lugdunensis* or *Staphylococcus saprophyticus* strains. Other modifications at the C-terminus of AgrA give rise to short extensions. However, these extensions result in a reduced or completely deficient *agr* phenotype.[40] Given the high degree of sequence conservation of the compound-binding site, it is reasonable to expect that any compound binding to this surface would be able to inhibit *agr* quorum sensing across all staphylococcal strains.

The fragment compounds identified in this study bind with millimolar affinity to the $AgrA_C$ protein. The low affinity reflects the small size of the compounds that populate the library used in the screen. Despite the low affinity of initial hits, fragment screening has previously been shown to provide a useful starting point for the development of higher-affinity inhibitors of protein−DNA interactions.[21,46] It is commonly observed that features of the original low-affinity fragment

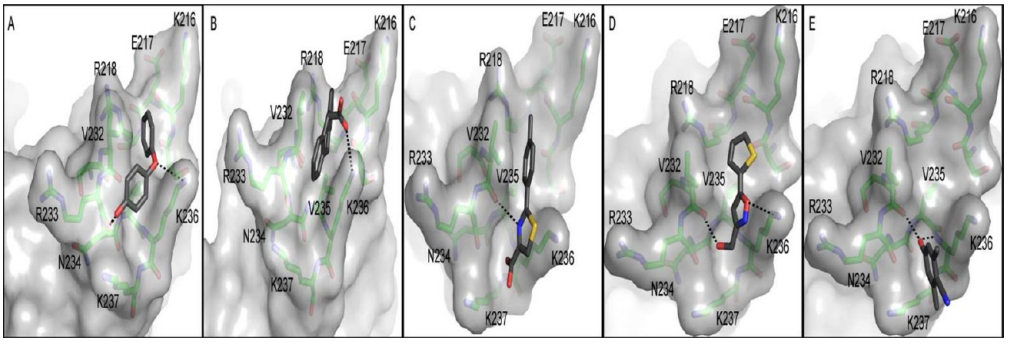

Figure 5. In silico compound docking predictions. Autodock Vina-predicted binding modes are shown for (A) 4-phenoxyphenol, (B) 9*H*-xanthene-9-carboxylic acid, (C) 2-(4-methylphenyl)-1,3-thiazole-4-carboxylic acid, (D) [5-(2-thienyl)-3-isoxazolyl]methanol, and (E) 4-hydroxy-2,6-dimethylbenzonitrile. Orientations of the protein are slightly different in each panel to optimize viewing of the predicted hydrogen bonds between the compound and protein, indicated by dashed lines.

dx.doi.org/10.1021/bi3011785 | *Biochemistry* 2012, 51, 10035−10043

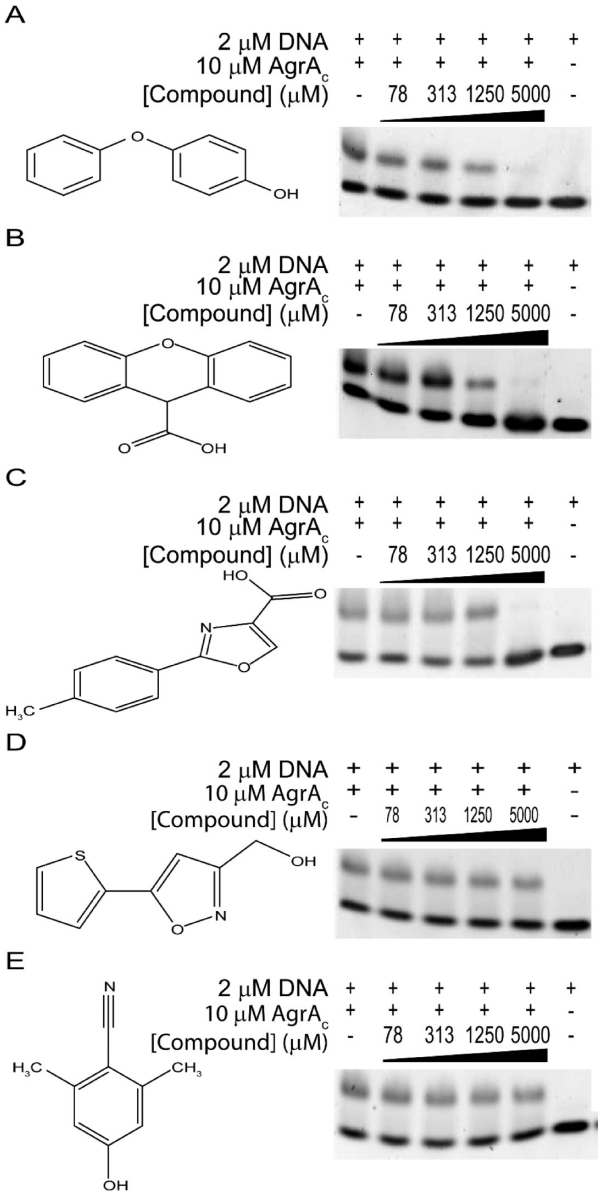

Figure 6. Effects of compounds on AgrA DNA binding activity. Electrophoretic mobility shift assays were performed with $AgrA_C$, its target DNA duplex, and the indicated concentrations of (A) 4-phenoxyphenol, (B) 9*H*-xanthene-9-carboxylic acid, (C) 2-(4-methylphenyl)-1,3-thiazole-4-carboxylic acid, (D) [5-(2-thienyl)-3-isoxazolyl]methanol, and (E) 4-hydroxy-2,6-dimethylbenzonitrile. DNA incubated with and without $AgrA_C$ in the absence of the compound are shown as positive and negative controls, respectively.

compound, identified by the initial screen, are maintained in the compounds that ultimately enter clinical development.[47−49] Further research is required to expand the pool of compounds that have been identified as AgrA inhibitors, to improve their affinity and specificity. The apo $AgrA_C$ crystal structure and NMR assignments that have been established here will provide valuable information to guide future compound development.

■ ASSOCIATED CONTENT

Accession Codes

The atomic coordinates and structure factors for apo $AgrA_C$ have been deposited in the Protein Data Bank. (entry 4G4K), and NMR resonance assignments have been deposited in the Biological Magnetic Resonance Bank (entry 18598).

■ AUTHOR INFORMATION

Corresponding Author

*Center for Advanced Biotechnology and Medicine, University of Medicine and Dentistry of New Jersey-Robert Wood Johnson Medical School, 679 Hoes Lane, Piscataway, NJ 08854-5627. Telephone: (732) 235-4844. E-mail: stock@cabm.rutgers.edu.

Funding

This work was supported in part by National Institutes of Health Grant R37 GM047958 to A.M.S. I.F.B. is supported in part by National Institutes of Health Graduate Training Grant GM008360.

Notes

The authors declare no competing financial interest.

■ ACKNOWLEDGMENTS

We thank G. V. T. Swapna for her assistance setting up the NMR experiments and G. T. Montelione for use of the NMR facility within the CABM Structural Bioinformatics Laboratory.

■ ABBREVIATIONS

AIP, autoinducing peptide; DMSO, dimethyl sulfoxide; DTT, dithiothreitol; NMR, nuclear magnetic resonance; NOE, nuclear Overhauser effect; PEG, polyethylene glycol; rmsd, root-mean-square deviation.

■ REFERENCES

(1) Talan, D. A., Krishnadasan, A., Gorwitz, R. J., Fosheim, G. E., Limbago, B., Albrecht, V., and Moran, G. J. (2011) Comparison of *Staphylococcus aureus* from skin and soft-tissue infections in U.S. emergency department patients, 2004 and 2008. *Clin. Infect. Dis. 53*, 144−149.

(2) Dohin, B., Gillet, Y., Kohler, R., Lina, G., Vandenesch, F., Vanhems, P., Floret, D., and Etienne, J. (2007) Pediatric bone and joint infections caused by Panton-Valentine leukocidin-positive *Staphylococcus aureus*. *The Pediatric Infectious Disease Journal 26*, 1042−1048.

(3) Kollef, M. H., and Micek, S. T. (2005) *Staphylococcus aureus* pneumonia: A "superbug" infection in community and hospital settings. *Chest 128*, 1093−1097.

(4) Petti, C. A., and Fowler, V. G., Jr. (2002) *Staphylococcus aureus* bacteremia and endocarditis. *Infectious Disease Clinics of North America 16*, 413−435 , x−xi.

(5) Todd, J., Fishaut, M., Kapral, F., and Welch, T. (1978) Toxic-shock syndrome associated with phage-group-I Staphylococci. *Lancet 2*, 1116−1118.

(6) European Centre for Disease Prevention and Control (2011) Antimicrobial resistance surveillance in Europe 2010. Annual Report of the European Antimicrobial Resistance Surveillance Network (EARS-Net), ECDC, Stockholm.

(7) Queck, S. Y., Jameson-Lee, M., Villaruz, A. E., Bach, T. H., Khan, B. A., Sturdevant, D. E., Ricklefs, S. M., Li, M., and Otto, M. (2008) RNAIII-independent target gene control by the *agr* quorum-sensing system: Insight into the evolution of virulence regulation in *Staphylococcus aureus*. *Mol. Cell 32*, 150−158.

(8) Koenig, R. L., Ray, J. L., Maleki, S. J., Smeltzer, M. S., and Hurlburt, B. K. (2004) *Staphylococcus aureus* AgrA binding to the *RNAIII-agr* regulatory region. *J. Bacteriol. 186*, 7549−7555.

(9) Janzon, L., Lofdahl, S., and Arvidson, S. (1989) Identification and nucleotide sequence of the δ-lysin gene, *hld*, adjacent to the accessory gene regulator (*agr*) of *Staphylococcus aureus*. *Mol. Gen. Genet. 219*, 480−485.

(10) Bronner, S., Stoessel, P., Gravet, A., Monteil, H., and Prevost, G. (2000) Variable expressions of *Staphylococcus aureus* bicomponent leucotoxins semiquantified by competitive reverse transcription-PCR. *Appl. Environ. Microbiol. 66*, 3931−3938.
(11) Dunman, P. M., Murphy, E., Haney, S., Palacios, D., Tucker-Kellogg, G., Wu, S., Brown, E. L., Zagursky, R. J., Shlaes, D., and Projan, S. J. (2001) Transcription profiling-based identification of *Staphylococcus aureus* genes regulated by the *agr* and/or *sarA* loci. *J. Bacteriol. 183*, 7341−7353.
(12) Janzon, L., and Arvidson, S. (1990) The role of the δ-lysin gene (*hld*) in the regulation of virulence genes by the accessory gene regulator (*agr*) in *Staphylococcus aureus*. *EMBO J. 9*, 1391−1399.
(13) Novick, R. P., Ross, H. F., Projan, S. J., Kornblum, J., Kreiswirth, B., and Moghazeh, S. (1993) Synthesis of staphylococcal virulence factors is controlled by a regulatory RNA molecule. *EMBO J. 12*, 3967−3975.
(14) Abdelnour, A., Arvidson, S., Bremell, T., Ryden, C., and Tarkowski, A. (1993) The accessory gene regulator (*agr*) controls *Staphylococcus aureus* virulence in a murine arthritis model. *Infect. Immun. 61*, 3879−3885.
(15) Booth, M. C., Atkuri, R. V., Nanda, S. K., Iandolo, J. J., and Gilmore, M. S. (1995) Accessory gene regulator controls *Staphylococcus aureus* virulence in endophthalmitis. *Invest. Ophthalmol. Visual Sci. 36*, 1828−1836.
(16) Gillaspy, A. F., Hickmon, S. G., Skinner, R. A., Thomas, J. R., Nelson, C. L., and Smeltzer, M. S. (1995) Role of the accessory gene regulator (*agr*) in pathogenesis of staphylococcal osteomyelitis. *Infect. Immun. 63*, 3373−3380.
(17) Mayville, P., Ji, G., Beavis, R., Yang, H., Goger, M., Novick, R. P., and Muir, T. W. (1999) Structure-activity analysis of synthetic autoinducing thiolactone peptides from *Staphylococcus aureus* responsible for virulence. *Proc. Natl. Acad. Sci. U.S.A. 96*, 1218−1223.
(18) Montgomery, C. P., Boyle-Vavra, S., and Daum, R. S. (2010) Importance of the global regulators Agr and SaeRS in the pathogenesis of CA-MRSA USA300 infection. *PLoS One 5*, e15177.
(19) Wright, J. S., III, Jin, R., and Novick, R. P. (2005) Transient interference with staphylococcal quorum sensing blocks abscess formation. *Proc. Natl. Acad. Sci. U.S.A. 102*, 1691−1696.
(20) Galperin, M. Y. (2008) Telling bacteria: Do not LytTR. *Structure 16*, 657−659.
(21) Hajduk, P. J., Huth, J. R., and Fesik, S. W. (2005) Druggability indices for protein targets derived from NMR-based screening data. *J. Med. Chem. 48*, 2518−2525.
(22) Sidote, D. J., Barbieri, C. M., Wu, T., and Stock, A. M. (2008) Structure of the *Staphylococcus aureus* AgrA LytTR domain bound to DNA reveals a β fold with an unusual mode of binding. *Structure 16*, 727−735.
(23) Otwinowski, Z., and Minor, W. (1997) Processing of X-ray diffraction data collected in oscillation mode. *Methods Enzymol. 276*, 307−326.
(24) McCoy, A. J., Grosse-Kunstleve, R. W., Adams, P. D., Winn, M. D., Storoni, L. C., and Read, R. J. (2007) Phaser crystallographic software. *J. Appl. Crystallogr. 40*, 658−674.
(25) Terwilliger, T. C. (2003) SOLVE and RESOLVE: Automated structure solution and density modification. *Methods Enzymol. 374*, 22−37.
(26) Emsley, P., and Cowtan, K. (2004) Coot: Model-building tools for molecular graphics. *Acta Crystallogr. D60*, 2126−2132.
(27) Adams, P. D., Afonine, P. V., Bunkoczi, G., Chen, V. B., Davis, I. W., Echols, N., Headd, J. J., Hung, L. W., Kapral, G. J., Grosse-Kunstleve, R. W., McCoy, A. J., Moriarty, N. W., Oeffner, R., Read, R. J., Richardson, D. C., Richardson, J. S., Terwilliger, T. C., and Zwart, P. H. (2010) PHENIX: A comprehensive Python-based system for macromolecular structure solution. *Acta Crystallogr. D66*, 213−221.
(28) Wishart, D. S., Bigam, C. G., Yao, J., Abildgaard, F., Dyson, H. J., Oldfield, E., Markley, J. L., and Sykes, B. D. (1995) ^{1}H, ^{13}C and ^{15}N chemical shift referencing in biomolecular NMR. *J. Biomol. NMR 6*, 135−140.
(29) Delaglio, F., Grzesiek, S., Vuister, G. W., Zhu, G., Pfeifer, J., and Bax, A. (1995) NMRPipe: A multidimensional spectral processing system based on UNIX pipes. *J. Biomol. NMR 6*, 277−293.
(30) Vranken, W. F., Boucher, W., Stevens, T. J., Fogh, R. H., Pajon, A., Llinas, M., Ulrich, E. L., Markley, J. L., Ionides, J., and Laue, E. D. (2005) The CCPN data model for NMR spectroscopy: Development of a software pipeline. *Proteins 59*, 687−696.
(31) Kay, L. E., Keifer, P., and Saarinen, T. (1992) Pure absorption gradient enhanced heteronuclear single quantum correlation spectroscopy with improved sensitivity. *J. Am. Chem. Soc. 114*, 10663−10665.
(32) Grzesiek, S., Dobeli, H., Gentz, R., Garotta, G., Labhardt, A. M., and Bax, A. (1992) ^{1}H, ^{13}C, and ^{15}N NMR backbone assignments and secondary structure of human interferon-γ. *Biochemistry 31*, 8180−8190.
(33) Farrow, N. A., Muhandiram, R., Singer, A. U., Pascal, S. M., Kay, C. M., Gish, G., Shoelson, S. E., Pawson, T., Forman-Kay, J. D., and Kay, L. E. (1994) Backbone dynamics of a free and phosphopeptide-complexed Src homology 2 domain studied by ^{15}N NMR relaxation. *Biochemistry 33*, 5984−6003.
(34) Furihata, K., Shimotakahara, S., and Tashiro, M. (2008) An efficient use of the WATERGATE W5 sequence for observing a ligand binding with a protein receptor. *Magn. Reson. Chem. 46*, 799−802.
(35) Mulder, F. A., Schipper, D., Bott, R., and Boelens, R. (1999) Altered flexibility in the substrate-binding site of related native and engineered high-alkaline *Bacillus* subtilisins. *J. Mol. Biol. 292*, 111−123.
(36) Trott, O., and Olson, A. J. (2010) AutoDock Vina: Improving the speed and accuracy of docking with a new scoring function, efficient optimization, and multithreading. *J. Comput. Chem. 31*, 455−461.
(37) Eletsky, A., Heinz, T., Moreira, O., Kienhofer, A., Hilvert, D., and Pervushi, K. (2002) Direct NMR observation and DFT calculations of a hydrogen bond at the active site of a 44 kDa enzyme. *J. Biomol. NMR 24*, 31−39.
(38) Fejzo, J., Lepre, C. A., Peng, J. W., Bemis, G. W., Ajay, Murcko, M. A., and Moore, J. M. (1999) The SHAPES strategy: An NMR-based approach for lead generation in drug discovery. *Chem. Biol. 6*, 755−769.
(39) Lepre, C. A., Peng, J., Fejzo, J., Abdul-Manan, N., Pocas, J., Jacobs, M., Xie, X., and Moore, J. M. (2002) Applications of SHAPES screening in drug discovery. *Comb. Chem. High Throughput Screening 5*, 583−590.
(40) Traber, K., and Novick, R. (2006) A slipped-mispairing mutation in AgrA of laboratory strains and clinical isolates results in delayed activation of *agr* and failure to translate δ- and α-haemolysins. *Mol. Microbiol. 59*, 1519−1530.
(41) Fowler, S. A., Stacy, D. M., and Blackwell, H. E. (2008) Design and synthesis of macrocyclic peptomers as mimics of a quorum sensing signal from *Staphylococcus aureus*. *Org. Lett. 10*, 2329−2332.
(42) Mansson, M., Nielsen, A., Kjaerulff, L., Gotfredsen, C. H., Wietz, M., Ingmer, H., Gram, L., and Larsen, T. O. (2011) Inhibition of virulence gene expression in *Staphylococcus aureus* by novel depsipeptides from a marine photobacterium. *Mar. Drugs 9*, 2537−2552.
(43) Otto, M., Sussmuth, R., Vuong, C., Jung, G., and Gotz, F. (1999) Inhibition of virulence factor expression in *Staphylococcus aureus* by the *Staphylococcus epidermidis agr* pheromone and derivatives. *FEBS Lett. 450*, 257−262.
(44) Geisinger, E., George, E. A., Muir, T. W., and Novick, R. P. (2008) Identification of ligand specificity determinants in AgrC, the *Staphylococcus aureus* quorum-sensing receptor. *J. Biol. Chem. 283*, 8930−8938.
(45) Jensen, R. O., Winzer, K., Clarke, S. R., Chan, W. C., and Williams, P. (2008) Differential recognition of *Staphylococcus aureus* quorum-sensing signals depends on both extracellular loops 1 and 2 of the transmembrane sensor AgrC. *J. Mol. Biol. 381*, 300−309.
(46) Hajduk, P. J., Dinges, J., Miknis, G. F., Merlock, M., Middleton, T., Kempf, D. J., Egan, D. A., Walter, K. A., Robins, T. S., Shuker, S. B., Holzman, T. F., and Fesik, S. W. (1997) NMR-based discovery of lead

inhibitors that block DNA binding of the human papillomavirus E2 protein. *J. Med. Chem. 40*, 3144−3150.

(47) Artis, D. R., Lin, J. J., Zhang, C., Wang, W., Mehra, U., Perreault, M., Erbe, D., Krupka, H. I., England, B. P., Arnold, J., Plotnikov, A. N., Marimuthu, A., Nguyen, H., Will, S., Signaevsky, M., Kral, J., Cantwell, J., Settachatgull, C., Yan, D. S., Fong, D., Oh, A., Shi, S., Womack, P., Powell, B., Habets, G., West, B. L., Zhang, K. Y., Milburn, M. V., Vlasuk, G. P., Hirth, K. P., Nolop, K., Bollag, G., Ibrahim, P. N., and Tobin, J. F. (2009) Scaffold-based discovery of indeglitazar, a PPAR pan-active anti-diabetic agent. *Proc. Natl. Acad. Sci. U.S.A. 106*, 262−267.

(48) Park, C. M., Bruncko, M., Adickes, J., Bauch, J., Ding, H., Kunzer, A., Marsh, K. C., Nimmer, P., Shoemaker, A. R., Song, X., Tahir, S. K., Tse, C., Wang, X., Wendt, M. D., Yang, X., Zhang, H., Fesik, S. W., Rosenberg, S. H., and Elmore, S. W. (2008) Discovery of an orally bioavailable small molecule inhibitor of prosurvival B-cell lymphoma 2 proteins. *J. Med. Chem. 51*, 6902−6915.

(49) Wyatt, P. G., Woodhead, A. J., Berdini, V., Boulstridge, J. A., Carr, M. G., Cross, D. M., Davis, D. J., Devine, L. A., Early, T. R., Feltell, R. E., Lewis, E. J., McMenamin, R. L., Navarro, E. F., O'Brien, M. A., O'Reilly, M., Reule, M., Saxty, G., Seavers, L. C., Smith, D. M., Squires, M. S., Trewartha, G., Walker, M. T., and Woolford, A. J. (2008) Identification of N-(4-piperidinyl)-4-(2,6-dichlorobenzoylamino)-1H-pyrazole-3-carboxamide (AT7519), a novel cyclin dependent kinase inhibitor using fragment-based X-ray crystallography and structure based drug design. *J. Med. Chem. 51*, 4986−4999.